

Carbon Dioxide degassing at Latera caldera (Italy): evidence of geothermal reservoir and evaluation of its potential energy

G. Chiodini ^{(a)*}, A. Baldini ^(b), F. Barberi ^(c), M. L. Carapezza ^(d), C. Cardellini ^(b), F. Frondini ^(b), D. Granieri ^(a), M. Ranaldi ^(c)

^a Osservatorio Vesuviano, INGV, via Diocleziano 328, 80124 Napoli, Italy

^b Dipartimento di Scienze della Terra, Università di Perugia, Piazza dell'Università, 06100 Perugia, Italy.

^c Dipartimento di Scienze Geologiche, Università di Roma Tre, Largo S. Leonardo Murialdo 1, 00146 Roma, Italy

^d Istituto Nazionale Geofisica e Vulcanologia, Sezione Roma 1, Via Vigna Murata 605, 00143 Roma, Italy

* Corresponding author

Abstract

In order to test the potentiality of soil CO₂ diffuse degassing measurements for the study of underground mass and heat transfer in geothermal systems detailed surveys were performed at Latera Caldera which is an excellent test site, due to the abundant available subsurface data. Over 2500 measurements of soil CO₂ flux revealed that endogenous CO₂ at Latera Caldera concentrates on a NE-SW band coinciding with a structural high of fractured Mesozoic limestones hosting a water-dominated high-enthalpy geothermal reservoir. The total hydrothermal CO₂ degassing from the structural high has been evaluated at 350 t d⁻¹ from an area of 3.1 km². It has been estimated that such a CO₂ release would imply a geothermal liquid flux of 263 kg s⁻¹, with a heat release of 239 MW. The chemical and isotopic composition of the gas indicates a provenance from the geothermal reservoir and that CO₂ is partly originated by thermal metamorphic decarbonation in the hottest deepest parts of the system and partly has a likely mantle origin. The ratios of CO₂, H₂, CH₄ and CO to Ar, were used to estimate the T-P conditions of the reservoir. Results cluster at T ~ 200-300°C and P_{CO₂} ~ 100-200 bars, close to the actual well measurements. Finally the approach proved to be an excellent tool to investigate the presence of an active geothermal reservoir at depth and that the H₂-CO₂-CH₄-CO-Ar gas composition is a useful T-P geochemical indicator for such CO₂ rich geothermal systems.

1. Introduction

In the last decades a great interest has been addressed to the CO₂ Earth degassing, mainly for studies related to the carbon global cycle [Allard *et al.*, 1991; Brantley and Koepenick, 1995; Kerrick *et al.*, 1995; Seward and Kerrick, 1996; Marty and Tolstikhin, 1998; Chiodini *et al.*, 2000, 2004a; Kerrick, 2001], and for the monitoring of active volcanoes [Chiodini *et al.*, 1996, 1998, 2001a, 2005; Hernandez *et al.*, 1998; Brombach *et al.*, 2001; Gerlach *et al.*, 2001; Salazar *et al.*, 2001; Frondini *et al.*, 2004; Granieri *et al.*, 2006]. These latter studies highlighted that CO₂ is mostly released from well defined areas, recently named Diffuse Degassing Structures (DDS, [Chiodini *et al.*, 2000]), related to recent tectonic and volcanic structures. Investigations of soil CO₂ degassing from geothermal areas have shown that frequently DDS are related to the underlying geothermal systems [Chiodini *et al.*, 1998; Bergfeld, *et al.*, 2001; Gambardella *et al.*, 2004; Werner and Cardellini, 2006]. Chiodini *et al.* [2000, 2004] showed that the Tyrrhenian side of the Italian peninsula is characterized by the presence of two large anomalies of deeply derived CO₂ degassing (Tuscan Roman Degassing Structure and Campanian Degassing Structure, TRDS and CDS respectively) releasing 1.4×10^{11} mol y⁻¹ and 0.7×10^{11} mol y⁻¹ of CO₂ respectively. In these areas, the CO₂ flux from depth is revealed at the surface by numerous discrete gas emissions, by zones of high soil diffuse degassing and by high CO₂ partial pressure (P_{CO₂}) in the groundwaters. In

particular, the TRDS region is also characterized by the occurrence of several, exploited or exploitable, geothermal systems of high (e.g., Larderello-Travale, Monte Amiata, Latera and Cesano), medium (e.g., Torre Alfina) and low (e.g., Viterbo) enthalpy are present. *Chiodini et al.* [1995] highlighted the strict correspondence, within TRDS, of CO₂ anomalies at the surface with buried carbonate horsts that act as gas traps and represent possible geothermal reservoirs.

The main objective of this work is to test the potentiality of soil CO₂ diffuse degassing measurements for the study of underground mass and heat transfer, and in particular for geothermal reservoir prospecting. In order to achieve this objective soil CO₂ flux surveys and gas sampling have been performed at Latera caldera, which is an outstanding case-study area for investigating the CO₂ diffuse degassing process and its relation to the tectonics and the geothermal system at depth. Latera caldera hosts one of the already discovered high enthalpy geothermal systems of Central Italy and its subsurface geology is well known thanks to a dozen of deep geothermal wells that have been drilled by the Energy National Agency (ENEL) and by the Geothermal Joint Venture ENEL-AGIP [*Barberi et al.*, 1984; *Bertrami et al.*, 1984].

2. Geological, hydrogeological and geothermal settings

Latera volcano, in the Vulsini complex, is the northernmost volcanic structure belonging to the Quaternary alkali potassic Roman Comagmatic Province (RCP [*Washington*, 1906]) that extends southwards up to the Vesuvius (Figure 1). In Pleistocene, Central Italy has been interested by extensive volcanism that is now attributed to the westward subduction of the Adriatic plate [*Doglioni et al.*, 1999; *Peccerillo*, 1985]. Many of the volcanic complexes of RCP, including Latera, exhibit a two-stage volcano-structural evolution (Figure 1) [*Acocella and Funiciello*, 2002]. In an early stage regional extension, mostly along NW-SE (Apenninic) faults, induced decompression and the rise of isotherms and magma. In a mature stage transverse NE-SW structures controlled the emplacement of magma chambers at upper crustal levels with magma extrusion in the volcanic belts of Central Italy and generation of high thermal anomalies at shallow depth (geothermal systems). Volcanoes are emplaced on a belt characterized by a series of mostly buried horsts and graben, well evidenced by gravity anomalies, that were mostly produced by extensional tectonics in Upper Miocene-Pleistocene, with marine clastic sedimentation in the structural lows [*Barberi et al.*, 1994].

The progressive eastward migration of the extension led to the formation of two distinct regions with different geological, geophysical and geothermal features. The western one, the Peri-Tyrrhenian region, is characterized by Pleistocene volcanism, a thinned crust (20-25 km), high heat flow (>80 mW m⁻² and up to 1000 mW m⁻² in the Larderello area) [*Baldi et al.*, 1992; *Della Vedova*

et al., 1984] and shallow earthquakes with moderate magnitude. The eastern one, the Apennine region, is to the contrary characterized by normal to high crustal thickness (30-40 km), low heat flow ($<40 \text{ mW m}^{-2}$ [Barchi *et al.*, 1998]) and deeper earthquake foci with higher magnitude.

Latera volcano developed on the western flank of the Bolsena caldera (Figure 2) and produced, mostly between 250 and 150 ka, several huge ignimbrite eruptions, with minor lavas and tephra, that in turn generated multiple collapses leading to the formation of the present complex polygenetic caldera that has an elliptic shape ($8 \times 10 \text{ km}$) with the major axis oriented NE-SW (Figure 2). The most recent volcanic activity occurred along NE-SW fissures in correspondence of a buried structural high with the same direction, revealed by gravimetric and drilling data [Barberi *et al.*, 1984]. The volcanic products of Latera cover the entire range of compositional variation from basic to evolved magmas of both the silica undersaturated high-K series (tephrite or leucitite to phonolites) and the silica saturated K series (trachybasalt to trachite) [Landi, 1987; Innocenti and Trigila, 1987; Tourbeville, 1993]. A syenitic body, intruded into carbonates, its dikes and the associated thermo-metamorphic rocks were encountered by wells drilled in the western part of the caldera at only 2 km depth from the surface [Durazzo *et al.*, 1982; Barberi *et al.*, 1984; Cavarretta *et al.*, 1985].

At Latera the volcanic products overlay a complex sedimentary sequence constituted by an allochthonous flysch (Ligurid unit), tectonically emplaced over a carbonate sequence (Tuscan series). Hydrogeology is characterized by the presence of a deep aquifer of regional importance hosted in the buried Mesozoic carbonate formations and by smaller and shallower aquifers hosted in the overlying volcanic rocks. The shallow and the deep aquifers are separated by low permeability rocks (flysch, marls, shale, argillitic altered volcanics) acting as aquicludes. The deep carbonate aquifer coincides with the geothermal reservoir while the Ligurid flysch represents the main cap rock of the system. The reservoir recharge occurs through infiltration and circulation of meteoric water in the Mesozoic carbonate rocks outcropping north and southwest of Latera caldera [Barberi *et al.*, 1984; Bertrami *et al.*, 1984; Cavarretta *et al.*, 1985; Chiodini *et al.*, 1995; Gianelli and Scandiffio, 1989]. The top of the main geothermal reservoir is located at 500-2000 m depth, its temperature ranges from 210°C to about 230°C (up to 343°C at 2775m depth in dry wells [Cavarretta *et al.*, 1985]) and the fluids are characterized by very high contents of carbon dioxide (about 0.7 mol kg^{-1} [Gambardella *et al.*, 2004]).

3. Methods

Three surveys of soil CO₂ diffuse degassing were performed on July and October 2003 within the Latera caldera (Figure 3) using the accumulation chamber method [Chiodini *et al.*, 1996, 1998] with a LI-820 infrared spectrometer as CO₂ detector. Gas discharged from the main vents (Figure 3) was sampled in August 2004 and July 2005. Four gas samples were collected in the Puzzolaie area (P1 to P4) and one in the area of an old sulphur mine (SM) following the procedure described by Chiodini [1994]. Puzzolaie is characterized by an intense soil degassing that is highlighted by a bare and altered soils and by bubbling in a small river while the emission at the sulphur mine is more localized and it is restricted to few small spots. The sampling was performed inserting a probe in the ground at shallow depth (0.2-0.7 m). At each site two samples were collected, one (total gas) using a 50 ml glass bottle, and one using a 250 ml glass bottle pre-evacuated and filled with about 50 ml of a 4N NaOH solution [Giggenbach, 1975; Giggenbach and Goguel, 1989]. The sampling procedure is described more in detail in Chiodini [1994].

Carbon dioxide and sulphur species, absorbed in the NaOH solution, were analyzed after oxidation with H₂O₂, by acid-base titration and by ion-chromatography, respectively. The non-absorbed gases (He, Ar, O₂, N₂, H₂, and CH₄), mainly present in the bottle headspace over the NaOH solution were analyzed by gas-chromatography. Carbon monoxide content and the CO₂ carbon isotopic composition were determined in the total gas sample by gas-chromatography and by mass-spectrometry respectively.

4. Geochemistry of the gas emissions

The composition of the Latera gas is reported in Table 1, also listing compositional data relative to gas together with that of the gas manifestations of the TRDS and of the fumarolic fluids of some Italian active volcanoes. The analyses show that CO₂ is the major component of Latera gas (~980,000 μmol mol⁻¹) followed by N₂, H₂S, CH₄, Ar, H₂, He and CO. Such a CO₂-rich composition is a common feature of the TRDS gases (Table 1). The processing of the geochemical data had a double objective: (i) to estimate temperature (T) and pressure (P) conditions of the system at depth through a gas-equilibria approach and (ii) to investigate the origin of the gas.

4.1. CO₂/Ar, H₂/Ar, CH₄/Ar and CO/Ar ratios as P-T ge indicators

The composition of gases from geothermal wells and fumaroles can be suitably used to investigate the reactions governing their origin and to obtain information on the T-P conditions of the source [Giggenbach, 1980; Chiodini and Marini, 1998]. However, in the case of low temperature surface gases this approach is hampered by the lack of information on the gas/steam ratio. To overcome this problem, Chiodini [1994] proposed a method involving only “dry” gases of

the system H₂-CO₂-CH₄-CO and considering CO₂ and C, represented by graphite, as the chemical species that control redox conditions in the sedimentary reservoirs hosting the geothermal systems of Central Italy. Another well known gas T-geoindicator is the couple H₂-Ar [Giggenbach, 1991]. This geothermometer is based on the dependence of f_{H_2} on T and on the assumption that Ar content of hydrothermal liquids equals that of air-saturated groundwater (ASW).

Here we re-consider these different approaches in order to derive new geoindicators based on the ratios CO₂/Ar, H₂/Ar, CH₄/Ar and CO/Ar. We assume that:

(I) the fugacity of H₂O (f_{H_2O}) is fixed by the presence of liquid water as:

$$\log f_{H_2O} = 5.51 - 2048/T \quad (1)$$

(II) the fugacity of CO₂ (f_{CO_2}) is not fixed by any reactions within the systems, but is an externally controlled variable. This is consistent with the evidence of reservoirs feeding gas emissions in TRDS acting as traps for CO₂ of deeper origin [Chiodini, 1994; Chiodini et al., 1995]. In these reservoir CO₂ can accumulate until saturation is reached and a free gas phase is formed at a pressure (either lithostatic or hydrostatic) controlled by depth;

(III) redox conditions are fixed either by the D'Amore and Panichi [D'Amore and Panichi, 1980] empirical relation:

$$\log f_{O_2} = 8.20 - 23643/T \quad (2)$$

which is generally valid for hydrothermal systems [Chiodini and Marini, 1998] or by the coexistence of CO₂ and organic matter [Chiodini, 1994] described by the relation:

$$\log f_{O_2} = 0.295 - 20713/T + \log f_{CO_2} \quad (3)$$

(IV) CO, H₂ and CH₄ are controlled by the following redox reactions:



According to the temperature dependence of their equilibrium constants, the fugacities of CO, H₂ and CH₄ (f_{CO} , f_{H_2} and f_{CH_4}) can be expressed as functions of T, f_{CO_2} , f_{H_2O} and f_{O_2} :

$$\log f_{\text{CO}} = 5.033 - 14955 / T - 0.5 \log f_{\text{O}_2} + \log f_{\text{CO}_2} \quad (7)$$

$$\log f_{\text{H}_2} = 2.548 - 12707 / T - 0.5 \log f_{\text{O}_2} \quad (8)$$

$$\log f_{\text{CH}_4} = 0.527 - 42007/T + \log f_{\text{CO}_2} + 2\log f_{\text{H}_2\text{O}} - 2\log f_{\text{O}_2} \quad (9)$$

The theoretical fugacities of CO, H₂ and CH₄ can be computed for any T- f_{CO_2} values, with f_{O_2} fixed either by equation 2 or 3. Because of the relatively low solubilities of the gases, the composition of the gas phase separated at depth will approach the composition of the gas dissolved in the liquid also at a low fraction of separated gas. The gas molar fractions in the liquid phase are related to the fugacities of the gases through the vapor – liquid distribution coefficient B_i [data from *Chiodini et al.*, 2001b]:

$$(X_i / X_{\text{H}_2\text{O}})_l = (X_i / X_{\text{H}_2\text{O}})_v / B_i \quad (10)$$

where $(X_i / X_{\text{H}_2\text{O}})_v$ is assumed $\sim f_i / f_{\text{H}_2\text{O}}$;

Finally we computed the ratios CO₂/Ar, H₂/Ar, CH₄/Ar and CO/Ar in the liquid phase by dividing $X_{i,l}$ values by the molar fraction of Ar in the liquid, assumed equal to that of ASW, i.e. $(X_{\text{Ar}} / X_{\text{H}_2\text{O}})_l = 3 \times 10^{-7}$.

The results of these computations are reported as T- P_{CO_2} (P_{CO_2} is considered $\sim f_{\text{CO}_2}$) grid lines in the diagrams log CH₄/Ar vs. log CO₂/Ar, log CO/Ar vs. log CO₂/Ar and log H₂/Ar vs. log CO₂/Ar (Figures 4 and 5), where the redox conditions fixed by either equation 2 [*D'Amore and Panichi*, 1980] or by the C-CO₂ redox buffer are considered, respectively. For the redox conditions fixed by the D'Amore and Panichi relation the ratios CO₂/Ar and CH₄/Ar are good indicator of P_{CO_2} as they are almost independent on T. The ratio H₂/Ar, which is independent on P_{CO_2} , is a good geothermometer, while the ratio CO/Ar is controlled by both T and P_{CO_2} . Considering instead the redox potentials buffered by the couple CO₂-C, all the ratios depend on both T and P_{CO_2} with the exception of CO₂/Ar which is mainly controlled by P_{CO_2} . Figures 4 and 5 can be used to graphically obtain from the compositions of Latera gases, independent estimations of T and P_{CO_2} . Excluding sample P2, which is air contaminated, the other samples form in all the diagrams a cluster at T of ~ 200 - 230°C and P_{CO_2} of ~ 100 - 200 bar. These T-P estimations are in fair agreement with the actual T- P_{CO_2} conditions of the geothermal reservoir of Latera, where a T of ~ 200 - 230°C was measured and a P_{CO_2} of ~ 100 bar was estimated [*Cavarretta et al.*, 1985].

The set of equations (1 – 10) above described can be used to compute the theoretical concentration of CO₂, CH₄, H₂, CO and Ar dissolved in the geothermal liquid at the reservoir conditions. Table 2 shows the computed composition for the well L2 fluid, which has a T of 212 °C and a P_{CO₂} of 100 bar [Cavarretta *et al.*, 1985], and for which analytical data of CO₂, CH₄ and H₂ are available [Chiodini, 1994]. The computed compositions are very similar to those measured in the well and reasonably similar to those measured in the surface emissions (Table 2) supporting the reliability of our geochemical approach. It is important to remark that at the T and P conditions of Latera geothermal system, the two redox assumptions, e.g. equation 2 [D'Amore and Panichi, 1980] and C-CO₂ give similar results (Table 2), as the same estimations of T and P_{CO₂} are obtained (Figures 4 and 5).

4.2. Origin of the Latera fluids

In order to characterize the origin of volatile components in relation to the tectonic setting, Giggenbach and Goguel [1989], Giggenbach [1987] and Giggenbach and Poreda [1993] proposed the use the relative concentrations of the inert gas constituents He, Ar, and N₂. Figure 6 plots the relative N₂, He, and Ar contents of Latera gases together with those of the other gas emissions of TRDS, of the active quiescent volcanoes of the Italian Peninsula (i.e. Vesuvius, Phlegrean Fields and Ischia) and of the potential end-member components.

Most of Latera samples show high N₂/Ar ratios (~ 1000) similarly to the other gas emissions of Central Italy testifying the absence of important air contamination, with the exception of the sample P2 that has the highest N₂ and Ar concentrations and a N₂/Ar ratio of 200 (Figure 6).

In general the gases from active volcanoes are relatively enriched in He while the TRDS gases, including the Latera ones, are richer in N₂. The N₂ enrichment is accompanied by a marked decrease in the ³He/⁴He ratios which lower from a Ra values of 2.5-3.5 in the active volcanoes to R/Ra values of 0.2-1.5 in the TRDS gases (Table 1). In particular Latera samples have R/Ra from 0.34 to 0.44. It is note worth that the ³He/⁴He ratios of the TRDS gases (0.035 R/Ra to 1.5 R/Ra; Table 1) overlap the range of ³He/⁴He ratios (0.44 R/Ra to 1.73 R/Ra) of fluid inclusions in olivines and pyroxenes phenocrysts of basic lavas and pyroclastic rocks from the RCP [Martelli *et al.*, 2004; Carapezza and Tarchini, 2006]. These low ³He/⁴He values of both magmatic fluid inclusions and gas emissions of RCP with respect to the “typical” mantle (³He/⁴He = 8 ± 1 R/Ra) would reflect the contamination of the mantle beneath Central Italy, driven by crustal fluids from the subducted Adriatic plate [Martelli *et al.*, 2004 and references therein].

Important N₂ contributions from thermal decomposition of organic matter recycled through subduction are thought to give rise to the relatively high N₂/Ar and N₂/He ratios of the TRDS gases.

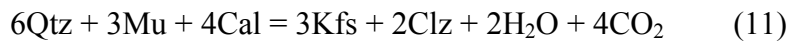
At a regional scale this picture is coherent also with the isotopic composition of CO₂; in fact typical TRDS gases have $\delta^{13}\text{C}$ values ranging from -4‰ to -2‰ vs PDB, which have been interpreted as the result of a mixing between a CO₂ produced at depth from carbonates and a more negative mantle CO₂ [Chiodini *et al.*, 2000, 2004a]. The carbon isotopic composition of the CO₂ emitted at Latera ($\delta^{13}\text{C}$ from $+1.5\text{‰}$ to $+2\text{‰}$) is significantly heavier than in the TRDS gases, suggesting the occurrence of local processes which cause the increase of the $^{13}\text{C}/^{12}\text{C}$ isotopic ratio. A possible cause for the ^{13}C enrichment could be CO₂ fractionation during steam generation. The CO₂ separated from liquid at T higher than 160°C is in fact heavier than the HCO₃⁻ in the parent solution [Friedman and O'Neil, 1977]. The gas geoindicators and the direct T measurements in deep wells, show that gases emitted at the surface are separated by a geothermal liquid rich in CO₂ at T of 200-230°C. We thus compute the carbon isotopic composition of the CO₂ generated by a single step separation process at this T and due to a pressure drop from 100 bar (the pressure estimated for the reservoir) to 1 bar (surface condition). In the computation we take into account the aqueous speciation of dissolved inorganic carbon, the total carbon mass balance and the isotopic carbon balance assuming isotopic equilibrium between H₂CO₃, HCO₃⁻, CO₃²⁻ and CO₂ according to the equations reported by Deines *et al.* [1974]. Speciation calculations were done with the software PHREEQC 2.10 [Parkhurst and Appelo, 1999]. Results show that H₂CO₃ is by far the main dissolved carbonate species and that fractionation between CO₂ and HCO₃⁻ is almost negligible and may account for a positive shift of $\delta^{13}\text{C}$ of less than 0.1 ‰. Consequently, steam generation can not account for the shift of 2-4 ‰ of Latera samples with respect to the most typical TRDS gases. We thus suggest that the high $\delta^{13}\text{C}$ values of Latera CO₂ derive from a partial contribution from metamorphic reactions involving silicate and carbonate minerals. The isotopic composition of the CO₂ produced by metamorphic decarbonation depends upon several factors but, as shown by Marini and Chiodini [1994], is generally more positive than the carbon of the protolites. The CO₂-calcite fractionation factor at relevant temperature (400-600°C) ranges from $+2.59\text{‰}$ to $+2.77\text{‰}$ [Ohmoto and Rye, 1979]; considering that $\delta^{13}\text{C}$ of protolites generally lies between 0 and $+2\text{‰}$ [Chiodini *et al.*, 2000] the carbon isotopic composition of metamorphic CO₂ is expected to be in the range from $+2.5\text{‰}$ to $+5\text{‰}$. The carbon isotopic composition of CO₂ emitted at Latera ($\delta^{13}\text{C}$ from $+1.5\text{‰}$ to $+2\text{‰}$) could then be explained by the mixing of this metamorphic CO₂ with the CO₂ of a regional deep (mantle) source characterized by $\delta^{13}\text{C}$ ranging from -4‰ to -2‰ .

The occurrence at Latera of metamorphic processes, at least in the past, is indicated by the presence of a metamorphic mineral assemblage at the contact between the syenitic body and the intruded limestone formations [Cavarretta *et al.*, 1985]. That metamorphic reactions persist

nowadays is supported by the high T measured by the geothermal wells in the deepest portion of Latera geothermal system.

A suitable tool to investigate this topic is the P_{CO_2} vs. $1000/T$ diagram of Figure 7 (adapted from *Chiodini and Marini* [1998] and *Chiodini et al.* [2001b]). In the diagram and in the following discussion the gas partial pressures are assumed equal to gas fugacities.

The diagram shows the T dependence of P_{CO_2} buffered by some thermo-metamorphic reactions. Figure 7 is revised from [*Chiodini and Marini*, 1998] to also include the line corresponding to the reaction:



which was suggested by *Gianelli* [1985] as the likely CO_2 -producing metamorphic reactions in the basement rocks of Central Italy. Any reaction can produce CO_2 at a given T only if P_{CO_2} is equal to or lower than the equilibrium value. Therefore, the position of the experimental data with respect to the equilibrium lines indicates whether or not metamorphic CO_2 production is possible.

In the diagram the data of Latera wells L1, L2, L3, L3d, L4, L5 and L6 are plotted. Direct P_{CO_2} and T measurements were available for the L2, L3d and L4 wells [*Gianelli and Scandiffio*, 1989], while for the other wells P_{CO_2} has been estimated as the difference between the total confining pressure (i.e., the hydrostatic pressure computed as $P_{\text{hydro}} = \rho_{\text{H}_2\text{O}} \times g \times z$, where $\rho_{\text{H}_2\text{O}}$ is the water density in kg m^{-3} at T conditions, g is 9.81 m s^{-2} , and z is the total well depth in m) and the water partial pressure ($P_{\text{H}_2\text{O}}$) at the bottom well T. In other words the presence of a CO_2 saturated liquid is assumed, for which $P_{\text{hydro}} = P_{\text{tot}} = P_{\text{CO}_2} + P_{\text{H}_2\text{O}}$. The $P_{\text{H}_2\text{O}}$ has been computed from $\log P_{\text{H}_2\text{O}} = 5.511 - 2046.7 / T^\circ\text{K}$ [*Giggenbach*, 1980], which refers to pure water, but can be used also for Latera geothermal water considering its relatively low salinity measured in the productive wells [*Gianelli and Scandiffio*, 1989]. Data in Figure 7 show that in most cases P_{CO_2} is too high to allow metamorphic CO_2 production. Only in the deep L1 well conditions would permit a metamorphic CO_2 production or its derivation from hydrothermal reaction as described by the full equilibrium function (line 4 in Figure 7), [*Giggenbach*, 1988]. These results suggest that the upper part of Latera geothermal system acts as a reservoir for CO_2 , while in its the deepest parts some CO_2 can be produced by thermal metamorphic reactions. In Figure 7, the data of the main geothermal systems of Central Italy are also reported. They show that the conditions for CO_2 generating thermo-metamorphic silicate-carbonate reactions are attained only at Larderello and Amiata geothermal systems, while the other geothermal systems of northern Latium have P_{CO_2} values that are 2-3

orders of magnitude higher than those required for a thermo-metamorphic CO₂ production within the reservoir.

5. Soil CO₂ diffuse degassing

Three soil CO₂ flux surveys were carried out at Latera caldera with different objectives. In July 2003, a first survey of 1089 measurements was performed mostly along the rural roads and in the vicinity of the geothermal wells (Figure 3) in order to screen the CO₂ degassing of the area and to compare CO₂ degassing from areas nearby productive geothermal wells with that from areas of unproductive wells. In the same period a detailed survey of 452 was performed at the Puzzolaie gas manifestation. In October 2003, a survey with a homogeneous measuring points distribution was performed in the SE sector of the caldera in order to collect a set of data suitable for a quantitative estimation of the CO₂ release. An area of 10.8 km² was surveyed with 930 CO₂ flux measurements (Figure 3). All surveys were carried out during periods of dry and stable atmospheric conditions. The data were elaborated using both statistical and geostatistical methods. A graphical statistical analysis (GSA method [Chiodini *et al.*, 1998]) was used to define background CO₂ fluxes vs. anomalous fluxes, while sequential Gaussian simulations method (sGs method [Deutsch and Journel, 1998]) was used to map the deeply derived CO₂ degassing process and to estimate the total release of CO₂ [Cardellini *et al.*, 2003].

5.1. The July 2003 survey

The soil CO₂ fluxes (ϕ_{CO_2}) measured in July 2003 are reported in the probability plot of $\log \phi_{\text{CO}_2}$ (Figure 8a). The ϕ_{CO_2} distribute in a wide range of values from 2.8 g m⁻² d⁻¹ to 53,000 g m⁻² d⁻¹ (average value of 278 g m⁻² d⁻¹) and plot along a complex curve which can be modeled as the combination of 3 log-normal ϕ_{CO_2} populations [Sinclair, 1974]: a population A with the highest values, an intermediate population B, and a population C with the lowest values. The statistical parameters of the individual partitioned populations, estimated by the Sichel *t*-estimator [David, 1977], are reported in Table 3. Population C can be interpreted reasonably as a background, ϕ_{CO_2} being in the range of CO₂ fluxes produced by a normal biological activity in the soil [Mielnick and Dugas, 2000; Rey *et al.*, 2002; Frank *et al.*, 2002; Yazaki *et al.*, 2004; Cardellini *et al.*, 2003]. The high ϕ_{CO_2} population A is clearly related to an endogenous CO₂ source. The high variability of this population ($\sigma = 0.78$) does not allow the use of the Sichel's tables [David, 1977] for the estimation of the mean ϕ_{CO_2} . The intermediate population B is most probably representative of a lower emission of endogenous CO₂.

A qualitative map of φ_{CO_2} distribution was derived applying the sGs procedure. To identify the areas with an anomalous CO_2 degassing, a probability map was derived from the results of the sGs (Figure 9). The map reports the probability, obtained from a large number of equiprobable realizations of the φ_{CO_2} spatial distribution (100 in this application), that at each location the flux be higher than a selected threshold [Cardellini *et al.*, 2003]. A value of $50 \text{ g m}^{-2} \text{ d}^{-1}$ was selected as a possible threshold for the background φ_{CO_2} on the base of the probability plot of Figure 8a. A more accurate definition of background φ_{CO_2} is discussed in the next section. The probability map of Figure 9 highlights that the surveyed area is characterized by a marked NE-SW elongated φ_{CO_2} anomaly and, in particular, that higher values are found near the productive geothermal wells L2, L3/3D, L4, L14, while no or very weak anomalies are detected in the surroundings of non-productive wells L1, L5 and L6.

In order to better constraint this promising finding and to quantify the CO_2 discharge by diffuse degassing, a more detailed survey was performed in October-November 2003 in the anomalous areas.

5.2. The October 2003 survey: mapping of soil CO_2 diffuse degassing and total CO_2 release estimation

Also the φ_{CO_2} of the October 2003 survey distribute in a wide range of values from $0.2 \text{ g m}^{-2} \text{ d}^{-1}$ to $2700 \text{ g m}^{-2} \text{ d}^{-1}$ (average value of $53 \text{ g m}^{-2} \text{ d}^{-1}$). The probability plot of φ_{CO_2} data (Figure 8b) shows again a complex statistical distribution that can be interpreted, also in this case, as a partial overlapping of three individual log normal populations whose statistical parameters are reported in Table 3. Because of its high mean values, the population A is clearly representative of CO_2 fluxes fed by an endogenous source [e.g., Chiodini *et al.*, 1998, 2001a; Cardellini *et al.*, 2003], while populations B and C are both compatible with a biogenic φ_{CO_2} . It is noteworthy that the population B of the October survey is very similar to the population C of the July survey. The presence of two low-flux populations in the October survey (populations B and C) could reflect either a combination of biological release with an endogenous flux component, or the diverse types of vegetation present in the surveyed area (e.g., grassland, cultivated field and forest). In general the larger fraction of low CO_2 fluxes of the October survey respect to the July one can reasonably depend on the different spatial distribution of the measurements and on the difference in the soil biological activity between the summer and the autumn season, especially in the sectors of the area used for agriculture. In particular during the October survey the wheat fields had been harvested.

With the objective to define a reasonable, unique threshold value for the background φ_{CO_2} , necessary to quantify the endogenous CO_2 flux component, a subset was selected of 193 measures

performed in an area far from the gas emissions (see Figure 10) and without macroscopic field evidences of anomalous CO₂ degassing. The φ_{CO_2} of the selected area ranges from 0.9 to 49 g m⁻² d⁻¹. The alignment of the subset data along a straight line in the probability plot (Figure 8b), indicates that the selected data represents a single statistically homogeneous population (i.e., log normal population). The estimated mean value for this subset is 15.7 g m⁻² d⁻¹ (95 % confidence interval 13.5 – 18.8 g m⁻² d⁻¹) and it can be assumed as a reasonable mean φ_{CO_2} background. This value is intermediate between the populations C and B, indicating that population B most probably derives from the combination of biological CO₂ release with a low magnitude endogenous flux component. Moreover, also the analysis of this data subset confirms that the value of 50 g m⁻² d⁻¹ can be reasonably considered as the maximum threshold for the biological φ_{CO_2} background.

Soil flux measurements of the October 2003 survey were used to draw a map of the soil CO₂ flux more detailed than that of July 2003. The experimental variograms of the normal scores of φ_{CO_2} (Figure 10) point out the presence of two nested structures characterized by a short range (410) and a long range (1850). These two structures can be referred to an anisotropy of the flux distribution with respect to the directions N45 (longer range) and N135 (shorter range) respectively (Figure 10). This finding is supported by the results obtained in the July survey. To perform the sGs, the experimental variograms of normal scores were modeled by the combination of two spherical variograms with nugget = 0.5, sill = 0.32 and range 410 m for the short range variogram, and with nugget = 0.5, sill = 0.18 and range = 1850 m for the long range variogram. One hundred simulations were computed by sGs considering a simulation cell of 10 m by 10 m, producing a set of equiprobable CO₂ flux distributions. The set was then post-processed to obtain the φ_{CO_2} map (Figure 11) and to estimate the total CO₂ output. The CO₂ flux map reports at any cell the mean CO₂ flux value obtained through a point-wise linear average of all the simulations.

The map of Figure 11 highlights the presence of several zones characterized by relatively high φ_{CO_2} (such as at Puzzolaie, P. Santa Luce, S. Martino, Sulphur Mine and a larger anomalous area between C. Fornacella, P. Paterno and F.na Cercone) limited by the geothermal wells L3/L3d and L4. The combination of these zones describes an anomalous degassing structure elongated NE-SW, according to the anisotropy of the flux distribution observed in the variograms. In the northern part of the study area the degassing zone is interrupted by a NW-SE oriented low CO₂ degassing zone separating the main anomaly from the small S. Martino and Sulphur Mine anomalies. Considering the value of 50 g m⁻² d⁻¹ as the maximum threshold for the biological CO₂ flux, the Latera DDS extends for about 3.1 km² (29 % of the surveyed area).

The CO₂ output from the surveyed area has been computed for each simulation by summing the products of the φ_{CO_2} value at each grid cell by the cell surface. The total CO₂ output is then

calculated by averaging the CO₂ output obtained for all the simulations. The associated standard deviation is assumed as the uncertainty of the estimation [Cardellini *et al.*, 2003]. The value obtained for the total CO₂ output is 497 t d⁻¹ (± 50 t d⁻¹). It is noteworthy that this estimation is affected by a relatively low uncertainty, being the standard deviation about 10 % of the estimated total CO₂ output. This result suggests both a good quality of the dataset and a suitable modeling of the φ_{CO₂} spatial distribution. Assuming the average background CO₂ flux previously reported (15.7 t d⁻¹ km²) for the entire surveyed area (10.8 km²), it is estimated that 169 t d⁻¹ of CO₂ are produced by biological activity, while 328 t d⁻¹ of CO₂ are of endogenous origin. This CO₂ flux represents a minimum estimation of the total amount of gas released at Latera by the deep source because the October 2003 campaign was designed to measure the soil diffuse emission of CO₂ over the entire caldera and not the emission from the anomalous areas of the gas manifestations. We refer here in particular at Puzzolaie, that is the biggest gas manifestation at Latera.

5.3. CO₂ diffuse degassing at Puzzolaie gas manifestation

Puzzolaie is characterized by the presence of numerous small gas vents, zones of alteration and areas of viscous flux of CO₂ resulting in a high small-scale spatial variability of soil degassing. In order to quantify the CO₂ emission from this area we used the data of the detailed soil φ_{CO₂} survey carried out in July 2003. The area of the gas manifestation (~52,000 m²) was investigated by means of 452 measurements with a measuring spacing of 5-10 m. Carbon dioxide fluxes range from 7.0 g m⁻² d⁻¹ to 25,240 g m⁻² d⁻¹ with an average value of 939 g m⁻² d⁻¹. In the probability plot of log φ_{CO₂} (Figure 8c) a good fitting of the observed probability distribution can be obtained with the partial overlapping of four different log normal φ_{CO₂} populations (populations A, B, C and D, Table 3). This high number of populations reflects the complexity of the CO₂ degassing process at Puzzolaie which is characterized by both different CO₂ sources (i.e., biological background and endogenous) and different types of flux (i.e., diffusive and viscous). For instance, in our interpretation the population of the lowest values (Population D) represents the background values while the population of the highest values (population A) reflects the highest flux of CO₂ from the endogenous source. The intermediate populations B and C could represent lower CO₂ flux from the endogenous source (population B), and a population composed by both the highest background values and the lowest φ_{CO₂} fed by the deep source (population C) respectively.

In spite of possible different interpretations of the origin of the populations, the CO₂ flux is almost entirely fed by the deep source. Ninety-eight % of the total CO₂ flux is in fact associated to Populations A and B. This estimation has been done computing the CO₂ output associated to each

population as $M_i \times f_i \times S$, where M_i and f_i are the φ_{CO_2} mean and the fraction of individual populations respectively, and S is the surface of the surveyed area.

The experimental variogram of Puzzolaie data (Figure 12a) differs from that of the entire data set of the October 2003 campaign (Figure 10): in particular data point to a lowest nugget effect (0.17) and a range value of 75 m indicating the presence of a local well defined small scale φ_{CO_2} anomaly. The map of φ_{CO_2} (Figure 12b), derived as the mean of 100 sequential Gaussian simulations, shows that also at a smaller scale the distribution of the φ_{CO_2} points out the presence of a NE-SW oriented anomaly consistent with the large scale φ_{CO_2} anomaly previously described.

The total CO_2 output from Puzzolaie area was estimated to 41 t d^{-1} ($\pm 2.9 \text{ t d}^{-1}$) which is about 20 t d^{-1} higher than the output from the same area estimated in the October 2003 survey. Being Puzzolaie the main gas manifestation of Latera, this result suggests that the contribution of discrete gas manifestations to the total output of CO_2 is relatively low respect to the gas emitted diffusively from the caldera. In any case, considering the emission at Puzzolaie, the total CO_2 output from Latera DDS is estimated to be $\sim 350 \text{ t d}^{-1}$.

6. Geothermal implications

Soil CO_2 flux surveys have shown that endogenous CO_2 degassing occurs only in the eastern part of Latera caldera from a NE-SW oriented structure. It is clear from the geophysical and drilling data [Barberi *et al.*, 1984; Bertrami *et al.*, 1984] that this degassing structure corresponds to a NE-SW trending structural high, consisting in a complex recumbent fold of the Tuscan limestones coupled with a tectonic overthrust over Ligurian flysch and limited by normal faults (Figure 13). On the structural high, the top of the limestones is at only a few hundred meters depth (-230 to -800 m below the surface) and it deepens both to the west (-1200 m) and to the east (-2000 m) with a corresponding increase of the thickness of the volcanic rocks and of the flysch deposits (Figure 13). The degassing structure coincides with the geothermal reservoir of Latera, where hydrothermal circulation is active as all the wells drilled on its top are productive (L2, L3/Ld, L4; Figure 9). It is important to remark that anomalous CO_2 degassing has been observed also outside the densely investigated area, in the proximity of wells L14 and L11, the latter located on the northern prolongation of the structural high (Figure 9) and where φ_{CO_2} values up to $140 \text{ g m}^{-2} \text{ d}^{-1}$, well above the background, have been measured. Both these wells found a pressurized CO_2 cap at the top of the limestones [Sabatelli and Mannari, 1995]. To the contrary, the wells located to the west (L1, L5, L6) or to the east (L10 planned to serve as a reinjection well, all drilled in zones where no evidence of endogenous CO_2 release has been found (Figure 9), proved not productive because they encountered hot but dry rocks, without permeability.

The reason for this strong difference in the permeability conditions at depth has to be found in the contrasting effects of mechanical rock fracturing by tectonic activity versus self-sealing processes induced by precipitation of hydrothermal minerals such as calcite and/or anhydrite at Latera geothermal system [Cavaretta et al., 1985]. In fact the zone of buried structural high displays geological evidence of recent and active faulting (see Figure 2) and is marked by a NE-SW alignment of earthquake epicentres [Buonasorte et al., 1987]. Calcite-anhydrite dissolution and precipitation processes in Central Italy geothermal systems are mainly controlled by P_{CO_2} variations [Marini and Chiodini, 1994]. For the conditions estimated for Latera reservoir, a reduction of P_{CO_2} can lead to the sealing of the system by anhydrite precipitation. In fractured zones as the Latera structural high, a sustained flux of deeply derived CO_2 maintains high P_{CO_2} in the reservoir that favors a “long life” of the geothermal system. Elsewhere, where tectonic fracturing is reduced, a low CO_2 flux from depth causes a P_{CO_2} decrease in the reservoir and its consequent progressive sealing by hydrothermal mineral deposition.

In any case, soil CO_2 flux surveys proved to be a very efficient tool to identify zones of high permeability at depth, e.g. the presence of geothermal reservoirs, as fluid leakage through faults tapping the reservoir, produces degassing anomalies recognizable at the surface.

On the base of T and P_{CO_2} estimations and taking into consideration the results of the geothermal wells [Bertrami et al., 1984], the following conceptual model for Latera geothermal system can be proposed. The fluid in the geothermal reservoir hosted in Mesozoic carbonate is mainly constituted by water and CO_2 and forms convective cells ascending toward the surface. Among the Latera’s productive wells, the one that better represents the reservoir conditions before degassing is L2 well (T= 212°C and P_{CO_2} = 100 bar; Cavaretta et al., 1985). At the top of the reservoir (500 m depth) T is 150°C (L3 well [Bertrami et al., 1984]) and P_{CO_2} is about 45 bar computed as the difference between P_{tot} and P_{H_2O} assuming a hydrostatic model. When total P equals hydrostatic P, a CO_2 -rich gaseous phase separates from the liquid and can accumulate at the reservoir top (wells L11 and L14) and/or be released toward the surface through the fractures of the system.

The CO_2 fluxes at the surface are mostly fed by degassing of the geothermal liquid. The total amount of liquid involved in the process, TL , can be expressed both as the ratio between the total heat content of the liquid W and its enthalpy H and as the ratio between the total output of CO_2 (F_{CO_2}) at the surface and $m_{CO_2,d}$ the molality of the degassed CO_2 at depth. In mathematical terms:

$$TL = \frac{F_{CO_2}}{m_{CO_2,d}} = \frac{W}{H} \quad (12)$$

If F_{CO_2} , $m_{CO_2,d}$, and H are known, equation 12 can be suitably used to compute both the total liquid (TL) and the total heat (W) involved in the degassing process of Latera geothermal system, which is an estimation of the geothermal energy associated with the fluid natural transfer within the system and consequently a minimum estimation of the geothermal potential of the area (i.e. the heat potentially released by the rocks during exploitation is not considered). An expression similar to equation 11 was used to estimate CO_2 flux from heat flow data at Taupo geothermal field, New Zealand [Kerrick *et al.*, 1995].

At Latera, the total CO_2 flux, F_{CO_2} , associated to hydrothermal degassing has been estimated in 350 t d^{-1} (92 mol s^{-1}) from an area of about 3.1 km^2 . The enthalpy of water H and the molality of degassed CO_2 , $m_{CO_2,d}$ can be computed assuming that T-P conditions of the well L2 ($T = 212^\circ\text{C}$ and $P_{CO_2}=100 \text{ bar}$ [Cavarretta *et al.*, 1985]) are representative of the system before degassing. According to the steam table of Keenan *et al.* [1969], the enthalpy of the liquid at 212°C is 907 J g^{-1} . The molality of degassed CO_2 , $m_{CO_2,d}$, has been computed assuming two different conditions. First we considered that all the CO_2 originally dissolved in the liquid phase ($m_{CO_2,t} = 0.72 \text{ mol kg}^{-1}$ at L2 well [Gambardella *et al.*, 2004]) is degassed to the surface. The resulting heat released by the system amounts to 116 MW, which represents a minimum estimate of the geothermal potential associated with the CO_2 degassing process, and the total liquid flux (TL) is 128 kg s^{-1} . If instead we assume more likely that degassing occurs along the uprising column of the convective cells, $m_{CO_2,d}$ is given by the difference between $m_{CO_2,t}$ and $m_{CO_2,r}$ the residual CO_2 still dissolved in the cooled descending liquid at the top of the convective cell (i.e. top of the reservoir). The $m_{CO_2,r}$ and $m_{CO_2,d}$ values are estimated to 0.37 mol kg^{-1} and to 0.35 mol kg^{-1} respectively, assuming the presence of a CO_2 saturated solution at the top of the reservoir ($T \sim 150^\circ\text{C}$, depth $\sim 500 \text{ m}$, $P_{CO_2} \sim 45 \text{ bar}$). In this case the resulting heat released by the system is 239 MW associated to a TL of 263 kg s^{-1} . The Latera geothermal plant has an installed electrical capacity of 26 MW (21 MW from double water flashing and 5 MW from binary cycle) and uses 5 production wells (L2, L2bis, L4, L4bis, L3d) and 5 reinjection wells located outside the caldera. At present the plant does not operate for environmental problems related to H_2S emission.

7. Conclusions

The Latera caldera hosts a water-dominated high enthalpy geothermal system. The geothermal reservoir is hosted in highly fractured Mesozoic carbonates forming a NE-SW elongated structural high. The reservoir fluid is a CO_2 -rich water at T of $200\text{-}300^\circ\text{C}$ and P_{CO_2} of $100\text{-}200 \text{ bars}$. Reservoir permeability is maintained by tectonic fracturing, as indicated by a relatively intense microseismicity and is favored by the high P_{CO_2} that prevents hydrothermal mineral precipitation

and sealing. Moving away from the structural high, underground T remains high but no permeability persists, likely because the reduced rock fracturation and the lower P_{CO_2} progressively sealed the original reservoir by calcite and anhydrite deposition, as indicated by the fractures filled with these hydrothermal minerals that are commonly encountered in the not-productive geothermal wells [Cavarretta *et al.*, 1985].

Cold gas emissions of mostly CO_2 occur at the surface along fractures above the buried structural high. Dry gases of the system $H_2-CO_2-CH_4-CO$ and their ratios to Ar, have been used to estimate the T-P conditions at depth, assuming two different redox conditions. Results reproduce the T-P values actually found in the geothermal reservoir by the wells and indicate that dry gases of cold manifestations can be conveniently used as T-P geoindicators when steam leaked from a geothermal reservoir totally condenses before reaching the surface.

The investigation of soil CO_2 flux proved useful to detect from the surface the presence of an active gas releasing geothermal reservoir at depth, as anomalous degassing of endogenous CO_2 has been found only above the structural high where all productive wells are located, CO_2 flux values being within the natural background of the area in the zones where no permeability at depth has been found.

From the soil flux survey, we estimated a total CO_2 release of 497 t d^{-1} , with a deeply derived CO_2 degassing of 350 t d^{-1} . The total amount of liquid associated to the diffuse degassing process (*TL*), range from 128 kg s^{-1} , if we consider that all the dissolved CO_2 is separated from the original liquid, to 263 kg s^{-1} considering that degassing occurs at the top of the reservoir and assuming the presence of a CO_2 saturated residual liquid solution. The thermal energy transported by the original liquid in the two different hypotheses is 119 and 239 MW respectively. These calculations indicate that LATERA geothermal system has an energy potential significantly higher than the present installed capacity (26 MWE); following this line of reasoning, the CO_2 soil flux maps of Figures 9 and 11 could help to locate new wells in sites with high probability of encountering the productive reservoir at depth.

Finally, geochemistry indicates that CO_2 is likely partly produced by thermal metamorphic decarbonation reactions, but it has also a relevant deep component of probable mantle origin, as in the other diffuse degassing structures of Central Italy [Chiodini *et al.*, 2004].

Acknowledgments.

We wish to thank J. Lewicki and A. Aiuppa for their constructive comments which were very useful to improve the manuscript. This work was made in the framework of the INGV-DPC V5 Project (2004-2006).

References

- Acocella, V., and R. Funiciello (2002), Transverse structures and volcanic activity along the Tyrrhenian margin of Central Italy, *Boll. Soc. Geol. It., spec. Vol. 1*, 739-747.
- Allard, P., et al. (1991), Eruptive and diffuse emissions of CO₂ from Mount Etna, *Nature*, 351, 387-391.
- Baldi, P., G. Bestini, and A. Ceccarelli (1992), Geothermal fields of Central Italy, paper presented at IGC, Kyoto, Japan.
- Barberi, F., F. Innocenti, P. Landi, U. Rossi, M. Saitta, R. Santacroce, and I. M. Villa (1984), The evolution of Latera caldera (Central Italy) in the light of subsurface data, *Bull. Volcanol.*, 47(1), 125-141.
- Barberi, F., et al. (1994), Plio-Pleistocene geological evolution of the geothermal area of Tuscany and Latium, *Mem. Descr. Carta Geol. It.*, 49, 77-134.
- Barbier, E., S. Bellani, and F. Musumeci (2000), The Italian geothermal database, paper presented at World Geothermal Congress, Japan.
- Barchi, M., G. Minelli, and G. Piali (1998), The CROP03 profile: A synthesis of results on deep structures of the Northern Apennines, *Mem. Soc. Geol. It.*, 52, 383-400.
- Bergfeld, D., F. Goff, and J. C. Janik (2001), Elevated carbon dioxide flux at the Dixie Valley geothermal field, Nevada; relations between surface phenomena and the geothermal reservoir, *Chem. Geol.*, 177, 43-66.
- Bertrami, R., G. M. Cameli, F. Lovari, and U. Rossi (1984), Discovery of Latera geothermal field: problems of the exploration and research, paper presented at Seminar on utilization of geothermal energy for electric power production and space heating, United Nation, Economic Commission for Europe, Florence, Italy.
- Brantley, S. L., and K. W. Koepenick (1995), Measured carbon-dioxide emissions from Oldoinyo-Lengai and the skewed distribution of passive volcanic fluxes, *Geology*, 23(10), 933-936.
- Brombach, T., J. C. Hunziker, G. Chiodini, C. Cardellini, and L. Marini (2001), Soil diffuse degassing and thermal energy fluxes from the southern Lakki plain, Nisyros (Greece), *Geophys. Res. Lett.*, 28(1), 69-72.
- Buonasorte, G., A. Fiordelisi, and U. Rossi (1987), Tectonic structures and the Vulsini volcanic complex, *Per. Mineral.*, 56, 123-136.
- Carapezza, M. L., and L. Tarchini (2006), Magmatic degassing of the Alban Hills volcano (Rome, Italy): geochemical evidence from accidental gas emission from shallow pressurized aquifers, *submitted to J. Volcanol. Geotherm. Res.*
- Cardellini, C., G. Chiodini, and F. Frondini (2003), Application of stochastic simulation to CO₂ flux

- from soil: Mapping and quantification of gas release, *J. Geophys. Res.*, *108*(B9), 2425-2437.
- Cavarretta, G., G. Gianelli, G. Scandiffio, and F. Tecce (1985), Evolution of the Latera geothermal system II: metamorphic hydrothermal mineral assemblages and fluid chemistry, *J. Volcanol. Geotherm. Res.*, *26*, 337-364.
- Chiodini, G. (1994), Temperature, pressure and redox conditions governing the composition of the cold CO₂ gases discharged in north Latium (Central Italy), *Appl. Geochem.*, *9*, 287-295.
- Chiodini, G., and L. Marini (1998), Hydrothermal gas equilibria: The H₂O-H₂-CO₂-CO-CH₄ system., *Geochim. Cosmochim. Acta*, *62*, 2673-2687.
- Chiodini, G., F. Frondini, and F. Ponziani (1995), Deep structures and carbon dioxide degassing in central Italy, *Geothermics*, *24*, 81-94.
- Chiodini, G., F. Frondini, and B. Raco (1996), Diffuse emission of CO₂ from the Fossa crater, Vulcano Island (Italy), *Bull. Volcanol.*, *58*(1), 41-50.
- Chiodini, G., R. Cioni, M. Guidi, B. Raco, and L. Marini (1998), Soil CO₂ flux measurements in volcanic and geothermal areas, *Appl. Geochem.*, *13*(5), 543-552.
- Chiodini, G., F. Frondini, C. Cardellini, F. Parello, and L. Peruzzi (2000), Rate of diffuse carbon dioxide Earth degassing estimated from carbon balance of regional aquifers: The case of central Apennine, Italy, *J. Geophys. Res.*, *105*(B4), 8423-8434.
- Chiodini, G., F. Frondini, C. Cardellini, D. Granieri, L. Marini, and G. Ventura (2001a), CO₂ degassing and energy release at Solfatara volcano, Campi Flegrei, Italy., *J. Geophys. Res.*, *106*, 16213-16221.
- Chiodini, G., L. Marini, and M. Russo (2001b), Geochemical evidence for the existence of high-temperature hydrothermal brines at Vesuvio volcano, Italy, *Geochim. Cosmochim. Acta*, *65* (13), 2129-2147.
- Chiodini, G., C. Cardellini, A. Amato, E. Boschi, S. Caliro, F. Frondini, and G. Ventura (2004a), Carbon dioxide Earth degassing and seismogenesis in central and southern Italy, *Geophys. Res. Lett.*, L07615, doi:07610.01029/02004GL019480.
- Chiodini, G., R. Avino, T. Brombach, S. Caliro, C. Cardellini, S. De Vita, F. Frondini, E. Marotta, and G. Ventura (2004b), Fumarolic degassing west of mount Epomeo, Ischia (Italy), *J. Volcanol. Geotherm. Res.*, *133*, 291-309.
- Chiodini, G., D. Granieri, R. Avino, S. Caliro, and A. Costa (2005), Carbon dioxide diffuse degassing and estimation of heat release from volcanic and hydrothermal systems, *J. Geophys. Res.*, *110*, B08204, doi:10.1029/2004JB003542.
- Collettini, C., C. Cardellini, G. Chiodini, N. De Paola, R. E. Holdsworth, and S. A. F. Smith (2007), Fault weakening due to CO₂ involvement in the extension of the Northern Apennines: short-

- and long-term processes. *J. Geol. Soc., Special Publication*, in press.
- D'Amore, F., and C. Panichi (1980), Evaluation of deep temperatures of hydrothermal systems by a new gas geothermometer, *Geochim. Cosmochim. Acta*, 44(3), 549-556.
- David, M. (1977), *Geostatistical ore reserve estimation*, 364 pp., Elsevier Scientific Publishing Company, Amsterdam.
- Deines, P., D. Langmuir, and R. S. Harmon (1974), Stable carbon isotope ratios and the existence of a gas phase in the evolution of carbonate ground waters, *Geochim. Cosmochim. Acta*, 38, 1147-1164.
- Della Vedova, B., G. Pellis, J. P. Foucher, and J. P. Rehaut (1984), Geothermal structure of Tyrrhenian Sea, *Mar. Geol.*, 55, 271-289.
- Deutsch, C. V., and A. G. Journel (1998), *GSLIB: Geostatistical Software Library and Users Guide*, second ed., 369 pp., Oxford University Press, New York Oxford.
- Doglioni, C., E. Gueguen, P. Harabaglia, and F. Mongelli (1999), On the Origin of westdirected subduction zones and applications to the western Mediterranean, in: *The Mediterranean Basins: Terziary Exstention within the Alpine Orogen. Geol. Soc. London, spec. issue* (156), 541-561.
- Durazzo, A., G. Bertini, U. Rossi, and A. Mottana (1982), Syenitic intrusions intersected by deep drilling at Latera, Vulsini Mountains, Latium, Italy., *N. Jahrb. f. Mineral. Abhandl.*, 145(3), 239-255.
- Federico, C., A. Aiuppa, P. Allard, S. Bellomo, P. Jean-Baptiste, F. Parello, and M. Valenza (2002), Magma-derived gas influx and water-rock interactions in the volcanic aquifer of Mt. Vesuvius, Italy, *Geochim. Cosmochim. Acta*, 66(6), 963-981.
- Frank, A. B., M. A. Liebig, and J. D. Hanson (2002), Soil carbon dioxide fluxes in northern semiarid grasslands, *Soil Biol. Biochem.*, 34, 1235-1241.
- Friedman, I., and J. R. O'Neil (1977), Compilation of stable isotope fractionation factors of geochemical interest, in *Data of Geochemistry, Sixth Edition, U.S. Geological Survey Profess. Paper 440-KK*, edited by M. Fleischer, p. 12, Washington D.C.
- Fron dini, F., G. Chiodini, S. Caliro, C. Cardellini, D. Granieri, and G. Ventura (2004), Diffuse CO₂ degassing at Vesuvio, Italy., *Bull. Volcanol.*, 66, 642-651.
- Fron dini, F., S. Caliro, C. Cardellini, G. Chiodini, N. Morgantini, and F. Parello (2006), Carbon dioxide degassing from Tuscany and Northern Latium (Italy). *Global Planet. Change* (in press).
- Gambardella, B., L. Marini, G. Ottonello, M. Vetusch i Zuccolini, C. Cardellini, G. Chiodini, and F. Fron dini (2004), Fluxes of deep CO₂ in the volcanic areas of central-southern Italy, *J.*

Volcanol. Geotherm. Res., 136, 31-52.

- Gerlach, T. M., M. P. Doukas, K. A. McGee, and R. Kessler (2001), Soil efflux and total emission rates of magmatic CO₂ at the Horseshoe Lake tree kill, Mammoth Mountain, California, 1995-1999, *Chem. Geol.*, 177(1-2), 101-116.
- Gianelli, G., and G. Scandiffio (1989), The LATERA geothermal system (Italy): chemical composition of the geothermal fluid and hypotheses on its origin., *Geothermics*, 18, 447-463.
- Giggenbach, W. F. (1975), A simple method for the collection and analysis of volcanic gas samples, *Bull. Volcanol.*, 39, 132-145.
- Giggenbach, W. F. (1980), Geothermal gas equilibria, *Geochimim. Cosmochim. Acta*, 44(12), 2021-2032.
- Giggenbach, W. F. (1987), Redox processes governing the chemistry of fumarolic gas discharges from White Island, New Zeland, *Appl. Geochem.*, 2, 143-161.
- Giggenbach, W. F. (1988), Geothermal solute equilibria. Derivation of Na-K-Mg-Ca geoindicators., *Geochim. Cosmochim. Acta*, 52, 2693-2711.
- Giggenbach, W. F. (1991), Chemical techniques in geothermal exploration., in *Application of geochemistry in geothermal reservoir development.*, pp. 119-142., UNITAR/UNDP, Rome.
- Giggenbach, W. F., and R.L. Goguel (1989), Collection and analysis of geothermal and volcanic water and gas discharges, 81 pp, Department of Science and Industrial Research, Chemistry Division, Petone, New Zealand
- Giggenbach, W. F., and R. J. Poreda (1993), Helium isotopic and chemical composition of gases from volcanic-hydrothermal systems in the Philippines., *Geothermics*, 22, 369-380.
- .Granieri, D., M. L. Carapezza, G. Chiodini, R. Avino, S. Caliro, M. Ranaldi, T. Ricci, and L. Tarchini (2006), Correlated increase in CO₂ fumarolic content and diffuse emission from La Fossa crater (Vulcano, Italy): Evidence of volcanic unrest or increasing gas release from a stationary deep magma body? *Geophys. Res. Lett.*, L13316, doi: 13310.11029/12006GL026460.
- Hernandez, P. A., N. M. Perez, J. M. Salazar, S. Nakai, K. Notsu, and H. Wakita (1998), Diffuse emission of carbon dioxide, methane, and helium-3 from Teide volcano, Tenerife, Canary Islands, *Geophys. Res. Lett.*, 25(17), 3311-3314.
- Innocenti, F., and R. Trigila (1987), Vulsini Volcanoes, *Periodico di Mineralogia*, 56 (spec. issue), 238 pp.
- Keenan, J. H., F. G. Keyes, P. G. Hill, and J. G. Moore (1969), *Steam-Tables - thermodynamic properties of water including vapor, liquid and solid phases (International edition metric units)*, 162 pp., Wiley, New York.

- Kerrick, D. (2001), Present and past nonanthropogenic CO₂ degassing from solid Earth, *Rev. Geophys.*, 39, 565-585.
- Kerrick, D. M., M. A. McKibben, T. M. Seward, and K. Caldeira (1995), Convective hydrothermal CO₂ emission from high heat-flow regions, *Chem. Geol.*, 121(1-4), 285-293.
- Landi, P. (1987), Stratigraphy and petrochemical evolution of Latera Volcano (Central Italy), *Per. Mineral.*, 56, 201-224.
- Marini, L., and G. Chiodini (1994), The role of carbon dioxide in the carbonate-evaporite geothermal systems of Tuscany and Latium (Italy), *Acta Vulcanol.*, 5, 95 -104.
- Martelli, M., P. M. Nuccio, F. M. Stuart, R. Burgess, R. M. Ellam, and F. Italiano (2004), Helium-strontium isotope constraints on mantle evolution beneath the Roman comagmatic province, Italy., *Earth Planet. Sci. Lett.*, 224(3-4), 295-308.
- Marty, B., and I. N. Tolstikhin (1998), CO₂ fluxes from mid-ocean ridges, arcs and plumes, *Chem. Geol.*, 145(3-4), 233-248.
- Metzeltin, S., and L. Vezzoli (1983), Contributi alla geologia del vulcano di Latera (Monti Vulsini, Toscana meridionale-Lazio settentrionale), *Mem. Soc. Geol. It.*, 25, 247-271.
- Mielnick, P. C., and W. A. Dugas (2000), Soil CO₂ flux in a tallgrass prairie, *Soil Biol. Biochem.*, 32, 221-228.
- Ohmoto, H., and R. A. Rye (1979), Isotopes of sulfur and carbon, in *Geochemistry of hydrothermal ore deposits 2d Ed.*, edited by H. L. Barnes, pp. 517-612, John Wiley, New York.
- Parkhurst, D. L., and C. A. J. Appelo (1999), User's guide to PHREEQC (version 2), A computer program for speciation, batch-reaction, one-dimensional transport, and inverse geochemical calculations, 312 pp, U.S. Geological Survey.
- Peccerillo, A. (1985), Roman comagmatic province. Evidence for subduction-related magma genesis, *Geology*, 13, 103-106.
- Rey, A., E. Pegoraro, V. Tedeschi, I. De Parri, P. G. Jarvis, and R. Valentini (2002), Annual variation in soil respiration and its components in a coppice oak forest in Central Italy, *Glob. Change Biol.*, 8, 851-866.
- Rogie, J. D., D. M. Kerrick, G. Chiodini, and F. Frondini (2000), Measurements of nonvolcanic CO₂ emission from some vents in central Italy., *J. Geophys. Res.*, 105(B4), 8435-8445.
- Sabatelli, F., and M. Mannari (1995), Latera development update, paper presented at World Geothermal Congress, Florence.
- Salazar, J. M. L., P. A. Hernandez, N. M. Perez, G. Melian, J. Alvarez, F. Segura, and K. Notsu (2001), Diffuse emission of carbon dioxide from Cerro Negro volcano, Nicaragua, Central America, *Geophys. Res. Lett.*, 28(22), 4275-4278.

- Seward, T. M., and D. M. Kerrick (1996), Hydrothermal CO₂ emission from the Taupo Volcanic Zone, New Zealand, *Earth Planet. Sci. Lett.*, 139(1-2), 105-113.
- Sinclair, A. J. (1974), Selection of threshold values in geochemical data using probability graphs, *J. Geochem. Explor.*, 3, 129 -149.
- Tedesco, D. (1996), Chemical and isotopic investigations of fumarolic gases from Ischia island (southern Italy): Evidences of magmatic and crustal contribution, *J. Volcanol. Geotherm. Res.*, 74(3-4), 233-242.
- Tedesco, D., and P. Scarsi (1999), Chemical (He, H₂, CH₄, Ne, Ar, N₂) and isotopic (He, Ne, Ar, C) variations at the Solfatara crater (southern Italy): mixing of different sources in relation to seismic activity. *Earth Planet. Sci. Lett.*, 171, 465-480.
- Turbeville, B. N. (1993), Petrology and petrogenesis of the Latera caldera, Central Italy, *J. Petrol.*, 34(1), 77-123.
- Washington, H. S. (1906), *The Roman comagmatic region*, 206-214 pp., Washington, D.C., Carnegie Institution of Washington.
- Werner, C., and C. Cardellini (2006), Comparison of carbon dioxide emissions with fluid upflow, chemistry, and geologic structures at the Rotorua geothermal system, New Zealand, *Geothermics*, 35, 221-238.
- Yazaki, Y., S. Mariko, and H. Koizumi (2004), Carbon dynamics and budget in a Miscanthus sinensis grassland in Japan, *Ecol. Res.*, 19, 511-520.

Figure captions

Figure 1. Geological and structural sketch of the Tyrrhenian margin of Central Italy [modified from *Acocella and Funicello, 2002*].

Figure 2. Structural sketch-map of Latera caldera: a) lava flows, b) travertine, c) tilted lacustrine deposits, d) lacustrine deposits, e) outcrops of the sedimentary substratum, f) caldera rim, g) faults and fractures, h) explosion crater, i) scoria cone, l) springs, m) thermal springs, n) gas emission, p) dip of structural surface, 1) Bolsena caldera rim, 2) Latera caldera rim, 3) Vepe collapse, 4) and 5) NE-SW and NW-SE structural lineaments [modified from *Metzelin and Vezzoli, 1983*].

Figure 3. Map of the study area with location of CO₂ flux measuring points, gas sampling points, geothermal wells, and trace of the geological cross section of Figure 13.

Figure 4. (a) plot of $\log(\text{CH}_4/\text{Ar})$ vs $\log(\text{CO}_2/\text{Ar})$, (b) $\log(\text{CO}/\text{Ar})$ vs $\log(\text{CO}_2/\text{Ar})$ (c) plot of $\log(\text{H}_2/\text{Ar})$ vs $\log(\text{CO}_2/\text{Ar})$. The theoretical P_{CO₂}-T grids assume that the redox conditions are fixed by the *D'Amore and Panichi [1980]* buffer.

Figure 5. (a) plot of $\log(\text{CH}_4/\text{Ar})$ vs $\log(\text{CO}_2/\text{Ar})$, (b) $\log(\text{CO}/\text{Ar})$ vs $\log(\text{CO}_2/\text{Ar})$ (c) plot of $\log(\text{H}_2/\text{Ar})$ vs $\log(\text{CO}_2/\text{Ar})$. The theoretical P_{CO₂}-T grids assume that the redox conditions are fixed by the CO₂ buffer.

Figure 6. He-Ar-N₂ triangle. The Latera gases (P1, P2, P3, P4, and SM) are compared with some other gases of central and southern Italy and with fumarolic gases of the Neapolitan active volcanoes.

Figure 7. Plot of P_{CO₂} vs T. Full circles refer to data measured at Latera wells; squares refer to values estimated for Latera wells as described in the text, considering temperatures of 343°C at 2775 m, 298°C at 2403 m, 300°C at 2500 m, and 222°C at 2004 m for L1, L3, L5, L6 wells respectively [*Barbier et al., 2000*]; open circles refer to data measured in some geothermal systems of central Italy [*Gambardella et al., 2004*]; dashed areas refer to the range of values reported for the high enthalpy geothermal systems of Larderello and Mt. Amiata [*Chiodini and Marini, 1998*]. The P_{CO₂}-T conditions of some relevant thermo-metamorphic reactions producing CO₂ are reported as 1) $\text{Cal} + \text{Qtz} = \text{Wo} + \text{CO}_2$, 2) $\text{Di} + 3\text{Dol} = 2\text{Fo} + 4\text{Cal} + 2\text{CO}_2$, 3) $\text{Dol} + 2\text{Qtz} = \text{Di} + 2\text{CO}_2$, 4) P_{CO₂}-T

“full equilibrium” function [Giggenbach, 1988], 5) $6\text{Qtz} + 3\text{Mu} + 4\text{Cal} = 3\text{Kfs} + 2\text{Clz} + 2\text{H}_2\text{O} + 4\text{CO}_2$ [Gianelli, 1985]. Reaction 1), 2) and 3) from Chiodini and Marini [1998] and references therein.

Figure 8. Probability plots of log CO₂ flux. The probability distributions of CO₂ flux (empty circles), the partitioned populations (dashed lines) and the theoretical combination of the partitioned populations (solid lines) are reported for the different surveys. a) July 2003 survey. b) October 2003 survey; also the CO₂ flux subset used to define the biological background flux is reported (diamonds). c) July 2003 Puzzolaie. The threshold value for the biological CO₂ flux ($50 \text{ gm}^{-2}\text{d}^{-1}$) is also shown.

Figure 9. Probability map of CO₂ flux (July 2003). The colors represent the probability that CO₂ flux is higher than $50 \text{ gm}^{-2}\text{d}^{-1}$ (i.e., of the biological background of CO₂ flux).

Figure 10. Experimental variogram and variogram model of normal score of CO₂ flux (empty circles). The directional variograms computed respect to the directions N45 (squares) and N135 (stars) are also shown.

Figure 11. Map of CO₂ flux (October 2003). The white line borders the Latera DDS, i.e. the area where CO₂ flux is higher than $50 \text{ g m}^{-2} \text{ d}^{-1}$. The red line borders the area including the CO₂ flux measurements (data subset) used to define the flux background (see text).

Figure 12. a) Experimental variogram and variogram model of normal scores of CO₂ flux of July 2003 Puzzolaie survey and b) map of the CO₂ flux of the area around the Puzzolaie gas manifestation.

Figure 13. Comparison between the surface CO₂ flux and a geological cross section of the geothermal system of Latera (modified after Barberi *et al.* [1984]). The trace of the section is indicated in Figure 3.

Tables

Table 1. Chemical and isotopic composition of gas emissions of Latera, TRDS and Neapolitan active volcanoes.

Sample	T (°C)	CO ₂	S _{tot}	Ar	O ₂	N ₂	CH ₄	H ₂	He	CO	δ ¹³ C _{CO2}	³ He/ ⁴ He
Latera												
SM	23.9	981000	1910	16.0	0.68	15900	1150	9.30	10.3	0.399	2.02	0.38
SM ^a	na	980000	1750	na	na	13000	900	2.63		0.10	na	na
P1	na	983992	6481	8.49	0.21	8573	936	3.59	5.72	0.346	na	na.
P2	20.2	981000	6650	56.5	0.00	11700	905	1.92	5.91	1.400	na.	0.34
P3	25.4	984000	6950	8.29	0.72	8430	925	9.30	5.91	0.346	1.58	0.44
P4	31.6	986000	4750	8.41	0.26	8295	994	9.46	6.13	0.150	1.53	0.44
Pu ^a	19	977000	6400	na	na	8420	844	4.20		0.05	na	na
TRDS gas emissions												
P.ggio Olivo ^b	na	986275	1177	10.9	1.99	7658	4853	19.3	3.99	0.083	0.2	na
C. di Manziana ^c	na	975441	12326	2.74	0.35	11961	225	42.5	0.893	0.253	-2.3	0.081
S. di Manziana ^c	na	965000	9850	138	2280	21000	12700	1.00	2.00	0.500	-4.1	na
Parco Mola ^b	na	966951	1469	12.0	0.53	11481	20059	22.5	4.48	0.133	0.1	na
Cava dei Selci ^c	na	988000	8950	22.3	4.00	2680	481	0.86	2.27	0.670	0.9	1.54
Solforata ^c	na	980000	10600	5.4	4.00	9347	109	0.07	9.28	0.530	-3.5	0.95
Salcheto ^d	na	970592	76	7.96	0.69	23978	5328	6.72	8.75	0.160	-4.8	na
Selvena ^c	na	885000	12500	12.3	0	17000	80400	17000	2.46	9.500	-3.4	0.414
Pienza ^c	na	942000	<5	45.0	676	36700	14400	2.00	12.0	0	-3.7	0.214
Rapolano Cecilia ^c	na	963000	0	7.78	0	32900	4090	3.37	15.0	0.350	-6.1	0.09
Bagni S. Filippo ^b	na	959183	1684	7.01	0.38	20185	18928	3.24	8.87	0.222	-2.3	na
Umbertide ^c	na	933830	664	16.1	1.17	63080	2352	8.58	47.1	0.164	-3.2	0.035
F.sso. Biscina ^b	na	985697	46	5.32	24.67	11528	2675	7.87	14.3	0.571	0.0	na
Fersinone ^b	na	949313	224	16.15	38.0	49681	665	4.09	57.4	0.227	na	na
San Faustino ^b	na	978940	523	37.33	154	16071	4264	0	8.67	1.581	0.6	na
Neapolitan active volcanoes												
Vesuvio ^c	95.6	981864	4642	2.86	2.34	1817	581	10689	4.38	385	0.06 ÷ 0.34	2.2 ÷ 2.7 ^h
Campi Flegrei ^f	158	985268	8665	3.61	0.89	3264	187	2601	8.32	3.39	-1.4 ÷ -1.7 ⁱ	2.5 ÷ 3.0
Ischia ^g	98.8	980867	9815	31.74	na	3763	59	5431	29.45	3.08	-3.5 ÷ -5.1 ^l	3.5 ÷ 3.9

Chemical composition are expressed as μmol/mol, carbon isotopic composition as ‰ vs. PDB, He isotopic composition as R/Ra = (³He/⁴He)_{sample}/³He/⁴He_{air}; na, not available.

^aData from Chiodini (1994); ^b data from Collettini *et al.* [2007]; ^c data from Rogie *et al.* [2000] and references therein; ^d data from Frondini *et al.* [2006]; ^e (mean value for gas composition) data from Chiodini *et al.* [2001b]; ^f (mean value for gas composition) data from Chiodini *et al.* [2001a, 2005] and references therein; ^g (mean value for gas composition) data from Chiodini *et al.* [2004b] and references therein; ^h data from Federico *et al.* [2002] and references therein; ⁱ Tedesco and Scarsi [1999] and references therein; ^l Tedesco [1996].

Compositions of gas from active volcanoes are recalculated on free H₂O basis.

Table 2. Comparison of computed and measured concentration of gases dissolved in the geothermal liquid of L2 well with the gas composition of surface manifestations.

Name	Type	P _{CO2} (bar)	T °C	CO ₂ (μmol/mol)	CH ₄ (μmol/mol)	H ₂ (μmol/mol)	CO (μmol/mol)	Ar (μmol/mol)
Latera L2 ^{a,b}	Well (measured)	100	212	945400	556	12.5	n.a.	n.a.
Latera L2 ^{a,b}	Well (calculated C-CO2)	100	212	998916	431	11.1	0.30	16.6
Latera L2 ^{a,b}	Well (calculated DP)	100	212	998735	587	12.0	0.32	16.6
SM	Gas emission (measured)	-	23.9	981000	1150	9.3	0.40	16.0
P2	Gas emission (measured)	-	20.2	981000	905	1.9	0.35	8.5
P3	Gas emission (measured)	-	25.4	984000	925	9.3	0.35	8.3
P4	Gas emission (measured)	-	31.6	986000	995	9.5	0.15	8.4

^aP_{CO2} and T from Cavarretta *et al.* [1985]; ^b compositional data from Chiodini [1994].

Table 3. Statistical parameters of partitioned CO₂ flux populations.

Population	f (fraction %)	M (mean g m ⁻² d ⁻¹)	95% confidence interval (g m ⁻² d ⁻¹)
<i>July 2003 survey</i>			
A	0.08	-	-
B	0.22	78.2	70.4-88.7
C	0.7	23.5	22.4-24.9
<i>October 2003 survey</i>			
A	0.07	449	348-632
B	0.83	29.4	27.6-34.2
C	0.10	4.3	3.77-4.58
<i>July 2003 Puzzolaie survey</i>			
A	0.10	6968	5951-8540
B	0.67	384	324-473
C	0.17	36.8	35.2-38.9
D	0.06	13.5	12.7-14.8